Light Metals 2013 *Edited by: Barry Sadler*
TMS (The Minerals, Metals & Materials Society), 2013

Light Metals 2013

ALUMINUM PROCESSING

Aluminum Processing II

Light Metals 2013 *Edited by: Barry Sadler*
TMS (The Minerals, Metals & Materials Society), 2013

THE EFFECT OF MAGNESIUM CONTENT ON MICROSTRUCTURE EVOLUTION DURING HOT DEFORMATION OF ALUMINUM ALLOYS

Trevor J. Watt[1], Shinya Yasuda[2], Koji Ichitani[2], Ken Takata[3], Alex Carpenter[4], Jakub Jodlowski[5] and Eric M. Taleff[1]

1. University of Texas at Austin, Mech. Engrg., 204 E. Dean Keeton St. C2200, Austin, TX 78712, USA
2. Furukawa-Sky Aluminum Corp., 1351 Uwanodai, Fukaya, Saitama 366-8511, Japan
3. Nippon Steel Corp., 20-1 Shintomi, Futtsu-city, Chiba 293-8511, Japan
4. Southwest Research Institute, P.O. Drawer 28510, San Antonio, Texas 78228, USA
5. Schlumberger Technology Center, 110 Schlumberger Drive, Sugar Land, Texas 77478, USA

Keywords: aluminum, magnesium, hot working, dynamic recrystallization, abnormal grain growth

Abstract: Aluminum alloy specimens were tested in tension and compression at temperatures up to 500 °C and strain rates up to 1.0 s^{-1} to study the microstructures developed during hot working. An AA5182 alloy was hot deformed in tension and subsequently annealed to promote recrystallization, while two Al-Mg alloys (Al-0.5Mg, Al-4.5Mg) were hot deformed in compression and examined as-quenched. The AA5182 alloy showed no signs of dynamic recrystallization, but experienced increased static recrystallization with increasing tensile strain during subsequent annealing. Annealing also resulted in static abnormal grain growth (SAGG) for the AA5182 in regions of light to moderate strain. The Al-4.5Mg alloy, which was tested at faster strain rates and in compression, showed signs of geometric dynamic recrystallization (GDRX) during deformation, while the Al-0.5Mg alloy did not show any signs of recrystallization under the same conditions. Results indicate that increased Mg concentration enhances GDRX and increases SAGG following hot deformation.

Introduction

Hot deformation is used to form aluminum alloys into simple product shapes, such as plate and sheet, and also into complicated shapes for the aerospace and transportation industries. The final strength of these products depends on the composition of the aluminum alloy, the processing conditions used to deform it, and subsequent heat treatments. The strength of aluminum alloys that cannot be precipitation strengthened, such as the Al-Mg 5000-series alloys, lies largely in the microstructure of the final product. This final microstructure is the result of grain rotation, grain distortion, recrystallization and grain growth during processing [1]. Recrystallization can occur dynamically during deformation or statically during subsequent heat treatment. Processing parameters strongly influence dynamic recrystallization (DRX). In the case of Al-Mg 5000-series alloys, increasing the strain, strain-rate, and temperature can all result in increased DRX [1].

Fine-grained AA5083 and similar alloys are used in superplastic forming operations at high temperatures and slow strain rates to form complex components. This deformation is primarily the result of grain-boundary-sliding (GBS) creep, which can result in plastic elongations over 300% [2-5]. Solute-drag (SD) creep is a different deformation mechanism that can be used to achieve the high elongations necessary to form complex parts. Although SD creep is active in Al-Mg alloys at lower temperatures and faster strain rates than is GBS creep, it produces a lower maximum elongation, typically around 100% [2-5]. However, SD creep does not require the fine-grained starting material that GBS creep does, which is a benefit for material cost. SD creep has the potential disadvantage of promoting abnormal grains during annealing following forming to large strains, and these can adversely affect product strength [6 - 11]. The mechanism identified for this process is static abnormal grain growth (SAGG) during annealing of a microstructure produced by the geometric dynamic recrystallization (GDRX) process during SD creep [8].

Static abnormal grain growth (SAGG) is the unstable growth of isolated grains, and can result in grain sizes on the order of the specimen dimensions. When annealing AA5182, the recrystallized grain structure is typically stable below 500°C, or unstable if annealing is above 500°C. The latter unstable grain structure results in SAGG [3, 8, 12]. However, SAGG is also possible for AA5182 below 500°C following hot deformation [6-8, 13]. SAGG can lead to significantly reduced local part strengths. SAGG may be prevented through alloying additions that promote the pinning of grain boundaries [6-7].

Al-Mg alloys generally have good formabilities, particularly at elevated temperatures [14]. However, Al-Mg alloys are susceptible to SAGG after hot forming, which can locally reduce yield strength by up to 50%. SAGG occurs in microstructures produced by the geometric dynamic recrystallization (GDRX) process, wherein subgrains are formed in a microstructure during hot deformation [15-18]. When the GDRX process is terminated prior to the "pinch-off" of individual subgrains by high-angle boundaries, this microstructure is then susceptible to SAGG during subsequent annealing [8].

Abnormal grain growth in Al-Mg alloys is, therefore, dependent on microstructure evolution during hot deformation. The role of Mg in microstructure evolution during hot deformation is explored in this study to better understand how to achieve microstructure refinement while avoiding SAGG. In this report, the hot deformation of three Al-Mg alloys is discussed. These are: (1) an AA5182 (Al-4.4Mg-0.36Mn-0.1Cu) tensile specimen, (2) an Al-0.5Mg compression specimen and (3) Al-4.5Mg compression specimen.

Experimental Procedures

The AA5182 tensile specimen was machined from a 3-mm-thick sheet material that was recrystallized to an equiaxed microstructure with a lineal-intercept grain size of 17 μm. The tensile coupon had a dog-bone geometry with the tensile axis parallel to the rolling direction, a gage length of 25 mm, a gage width of 6 mm, a shoulder radius of 3 mm, and a thickness equal to that of the as-received sheet. Tensile testing was performed using a computer-controlled, electromechanical test system. Temperature was specified in an air-circulated resistance furnace and monitored with a type-K thermocouple in contact with the specimen gage region. The specimen was tested in tension until rupture at a true-strain rate of 3×10^{-2} s^{-1} and a temperature of 400°C and was then immediately quenched into water. Half the specimen was subsequently annealed for approximately 1 hour at 400°C.

The Al-0.5Mg and Al-4.5Mg materials were produced by direct-chill casting followed by homogenizing to achieve approximately equiaxed microstructures with average lineal intercept grain sizes of approximately 100 μm. After homogenization, the specimens were machined into cylinders 12 mm long and 8 mm in diameter. These specimens were mechanically upset to a final height of approximately 6 mm at 500°C and a strain rate of 1.0 s^{-1}. The specimens were quenched in He gas immediately after upsetting. A summary of all the testing conditions for the specimens is provided in Table 1.

After testing, the specimens were mounted in epoxy for metallographic preparation and examination. Each specimen was sequentially ground with 500, 1200 and 4000 grit SiC papers, and then sequentially polished with 3-μm and 1-μm diamond suspensions. Final polishing used a 0.04-μm colloidal silica suspension. Electrolytic etching of polished specimens for subsequent optical microscopy used Barker's reagent (5 mL HBF_4 in 100 mL H_2O) for 90 seconds at 25 V.

Optical photomicrographs were digitally acquired across contiguous areas of each specimen using polarizing filters with a sensitive tint (λ plate) to reveal the microstructure in color. These images were stitched together in software to produce a composite high-resolution image spanning a large area of interest for each specimen.

Results and Discussion

Figure 1 shows a mosaic image of the AA5182 tension specimen after deformation and annealing. There is a gradual decrease in specimen height from right to left. This decreasing height corresponds to an increasing strain from right to left, as a result of necking. The far left side of the image shows the final rupture site. As local strain increases, from right to left, the number of nucleation sites for recrystallization increases, resulting in a finer recrystallized microstructure. Thus, the finest recrystallized grains are present near the rupture site where strains are greatest. Farther right, the less-strained regions result in larger grains because of fewer nucleation sites. The very largest grains, which can span more than half the height of the specimen, are the result of SAGG.

Figure 2 shows a mosaic image of the as-quenched Al-0.5Mg upset sample. Barreling is evident, which is the result of friction between the specimen and die surfaces. Grains in the center region near the contacting surfaces are generally equiaxed. Lineal-intercept grain size measurements (ASTM E112) provide an average grain size of 131 ± 18 μm in this region. Based on the original grain size of 100 μm, there appears to be uniform grain growth, but no recrystallization, in this region. Grains in the center of the specimen are highly deformed, exhibiting elongation in the horizontal direction. This is consistent with the expected plastic deformation at the specimen center, away from the friction constraints at the specimen-die interfaces. Measurements at the center of the specimen produced a mean grain size of 189 ±38 μm, with an aspect ratio (length/height) of approximately 4.0. This larger grain size may be the result of grain growth, compounded by plastic heating generated during deformation. However, the irregular nature of the deformed grains in the central region certainly introduces errors into results of the lineal intercept method. Image-based area and perimeter calculations may be better suited to this region.

Table 1: Specimen Compositions and Test Conditions

	Alloy Composition (wt.%)									Deformation	Post-Deformation
Alloy	Si	Fe	Cu	Mn	Mg	Cr	Zn	Ti	Al	Conditions	Heat Treating
AA5182	0.11	0.18	0.100	0.36	4.40	0.04	0.020	0.02	bal.	400°C, 0.03 s^{-1}	400°C, 1 hour
Al-0.5Mg	0.10	0.11	0.002	0.05	0.50	0.05	0.006	0.01	bal.	500°C, 1.00 s^{-1}	None
Al-4.5Mg	0.11	0.11	0.004	0.05	4.39	0.05	0.004	0.01	bal.	500°C, 1.00 s^{-1}	None

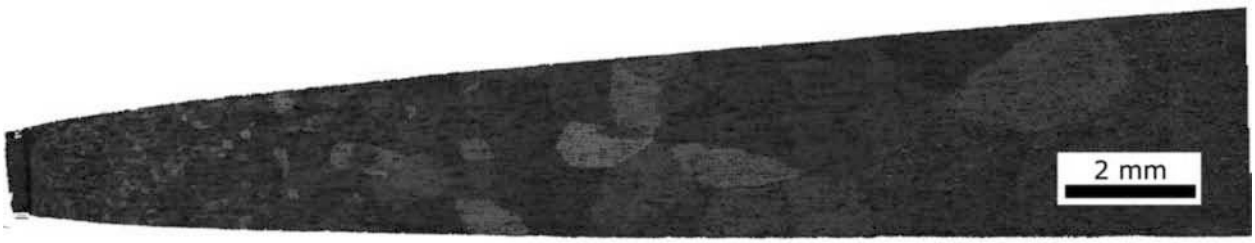

Figure 1: This figure shows refinement from hot deformation of AA5182 as well with RX and SAGG. Specimen tested in tension at 400°C and 3×10^{-2} s^{-1} and subsequently annealed at 400°C for 1 hour.

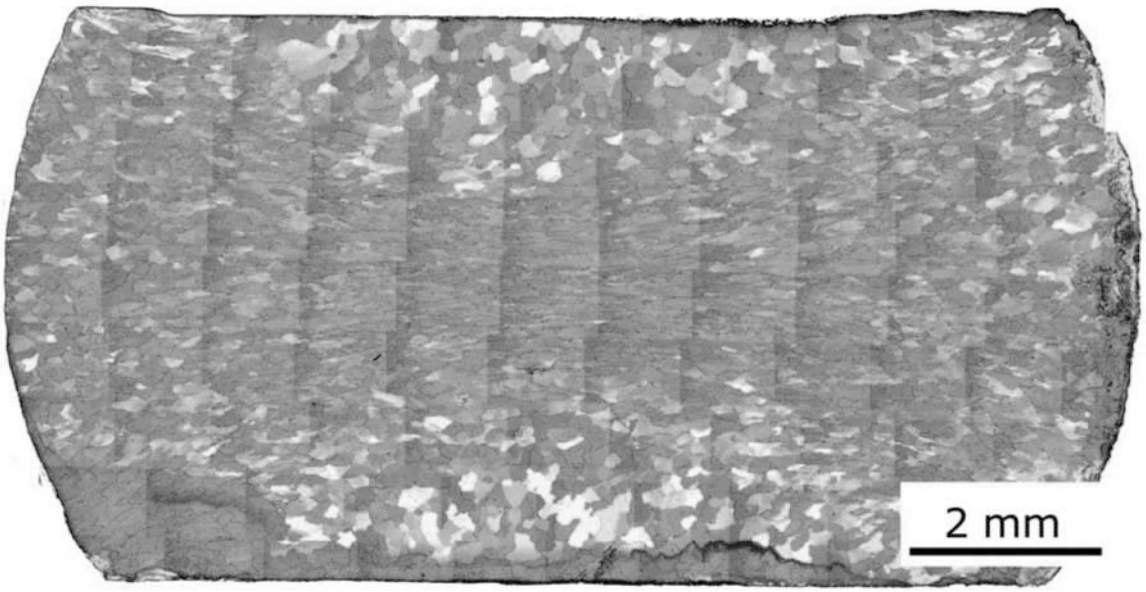

Figure 2: A mosaic image is shown for the Al-0.5Mg specimen, upset at 500°C and 1.0 s^{-1}. The height of the specimen is 6.00 mm.

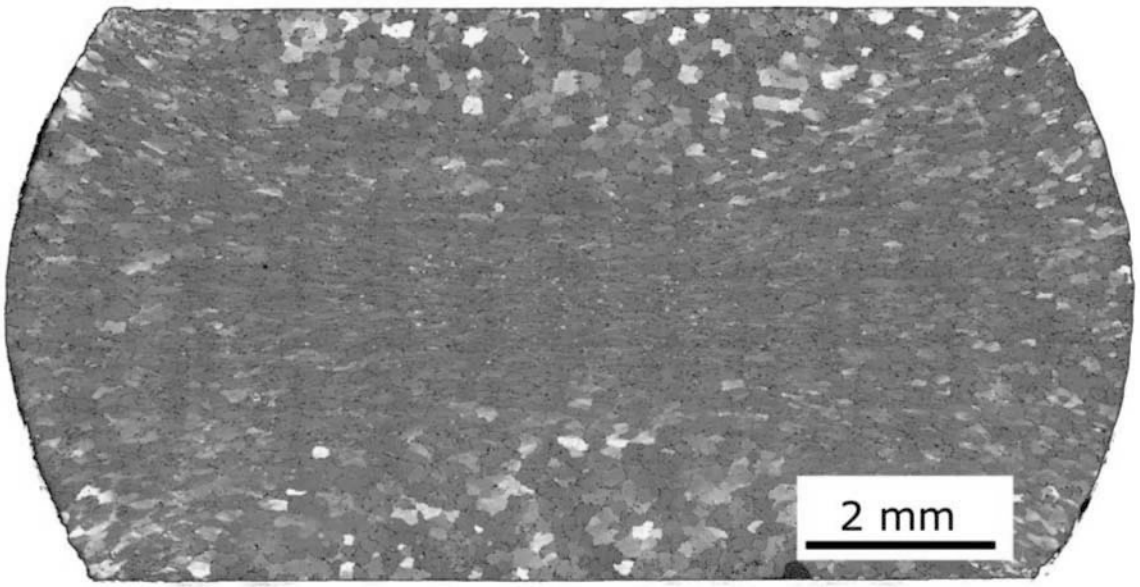

Figure 3: A mosaic microscope image is shown for the Al-4.5Mg specimen, upset at 500°C and 1.0 s^{-1}. The height of the specimen is 6.05 mm.

Figure 3 shows a mosaic image of the upset Al-4.5Mg specimen. As in the Al-0.5Mg specimen, there are characteristic equiaxed microstructures near the contacting die surfaces, and a central region of highly deformed grains. The mean grain size of the Al-4.5Mg specimen near the die contacts is 131 ±15 μm, which is similar to that of the Al-0.5Mg specimen. In the specimen center, the mean grain size is 100 ±18 μm, and the average grain aspect ratio is 2.5, much less than the Al-0.5Mg specimen. The finer grain size at the center of the Al-4.5Mg specimen, compared to the Al-0.5Mg specimen, is likely the result of different deformation mechanisms promoted by a larger Mg content. A summary of the grain size measurements for the Al-0.5Mg and Al-4.5Mg alloys is provided in

Table 2.

Table 2: Grain Size Measurements for Al-0.5Mg and Al-4.5Mg

Alloy	Location	Horizontal Grain Size (μm)	Vertical Grain Size (μm)	AR* (H/V)
Al-0.5Mg	Top	132 ± 17	130 ± 19	1.01
	Center	303 ± 62	76 ± 15	4.00
Al-4.5Mg	Top	143 ± 16	119 ± 15	1.20
	Center	143 ± 30	57 ± 7	2.49

* AR = aspect ratio (AR = H/V) , V = vertical (height) grain size, H = horizontal (radial) grain size

Figure 4 shows higher-magnification images of the top-center contact surfaces in the Al-0.5Mg and Al-4.5Mg specimens. Both microstructures show some residual denritic structure in the individual grains, which would be expected to become more pronounced with additional etching [19]. There is greater pitting observed in the Al-4.5Mg sample along grain boundaries and at the residual dendrite boundaries. This is likely from the formation of intermetallic compounds (IMCs) that preferentially nucleate at grain boundaries and between dendrite arms [14], leading to galvanic reactions that promote pitting during etching. The Al-4.5Mg alloy has nine time more Mg than does the Al-0.5Mg, which will produce more Mg-associated IMCs.

Figure 5 shows higher magnification images of the middle region in each Al-Mg specimen. The most obvious difference between the two microstructures is the presence of equiaxed, recrystallized grains in the Al-4.5Mg alloy. Because the specimens were immediately quenched with He after testing, the presence of recrystallized grains might be interpreted as the result of DRX. However, the evidence for this is not conclusive, as the quench rate may have been insufficient to prevent static recrystallization followin deformation. It is worth considering the different mechanisms that might have produced these equiaxed, recrystallized grains.

The as-quenched AA5182 tensile specimen, the microstructure of which was examined but is not shown here, did not contain any evidence of DRX. Recrystallization was only evident following static annealing after hot deformation. The absense of recrystallized grains is conclusive that DRX did not occur in the AA5182 material. Because the Mg contents of the AA5182 and Al-4.5 Mg materials are quite similar, it is natural to expect similar behaviors between these two materials. Thus, one mechanism worthy of consideration is static recrystallization from nuclei produced by GDRX during hot deformation, as demonstrated in Figure 1 for the AA5182 specimen. The higher test temperature of the Al-4.5Mg specimen, 500 *versus* 400°C, would promote recrystallization and increase the quench rate required to supress static recrystallization or SAGG. However, this is not the only explanation that should be considered for the equiaxed, recrystallized grains that form in the Al-4.5Mg specimen. The greater Mg content of the Al-4.5 Mg material would also be expected to suppress recovery during deformation, which is part of the reason that Mg promotes GDRX in Al-Mg alloys. The recrystallized grains in the Al-4.5Mg generally occur along the boundaries of deformed grains. Such recrystallization, sometimes described as a "pearl necklace" morphology, may simply be the result of sufficient local deformation along boundaries to induce dynamic recrystallization. Intermetallic particles along the boundaries might also promote such a recrystallization structure through particle-stimulated nucleation or recreystallization, but it is not clear how an increased Mg content could promote this mechanism, as all Mg should be in solid-solution at the deformation temperatures investigated.

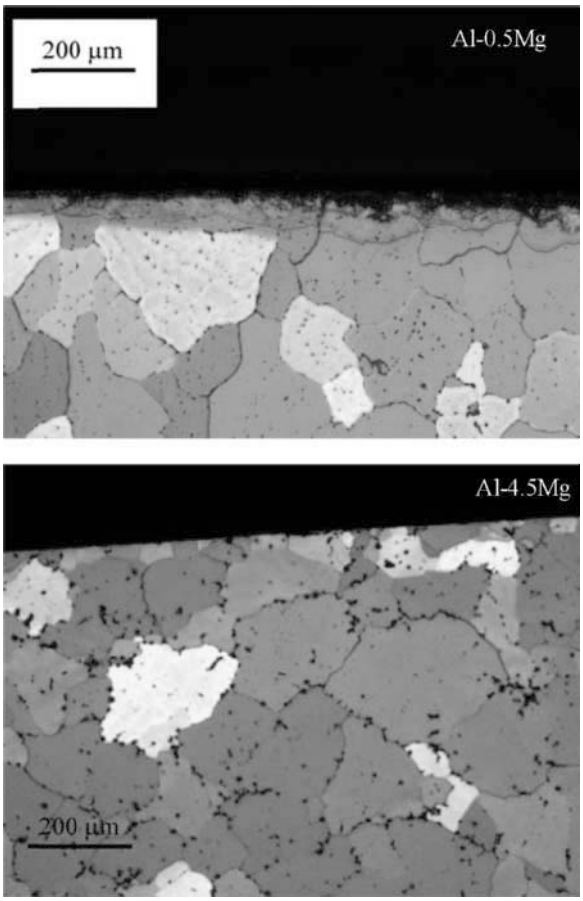

Figure 4: Grain morphologies are shown at the top-center of specimens. The radial direction is horizontal, and the length direction is vertical.

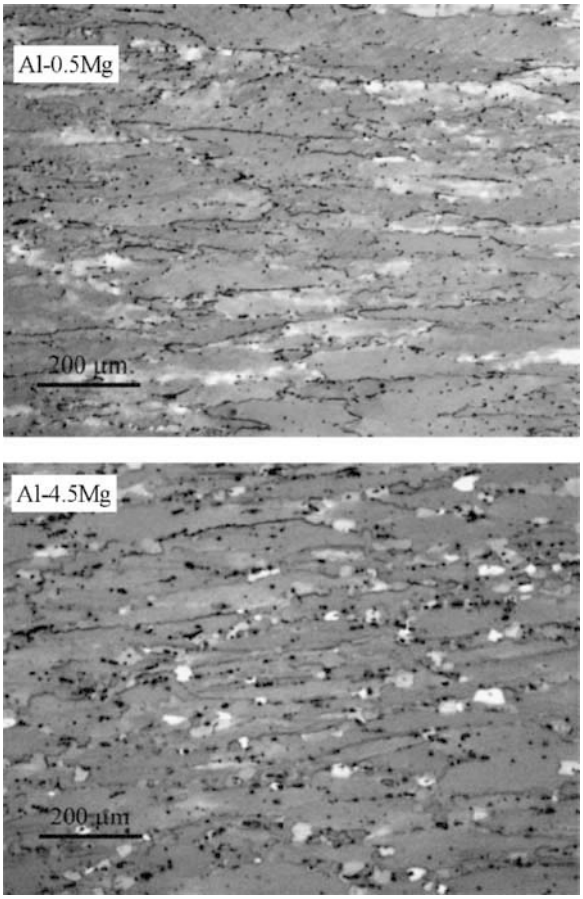

Figure 5: Grain morphologies are compared for the middle-center of specimens. The radial direction is horizontal, and the length direction is vertical.

Conclusions

The addition of magnesium promotes static and potentially dynamic recrystallization (DRX) in hot-worked Al-Mg alloys. The increase in DRX increases the likelihood of static abnormal grain growth (SAGG) following hot deformation, which is detrimental to final part strength. Recrystallization associated with increased Mg content may also enhance microstructure refinement during hot deformation, as demonstrated by the Al-4.5Mg specimen in comparison to the Al-0.5Mg specimen.

Acknowledgements

This work was funded in part by the National Science Foundation's Division of Materials Research Award DMR-1105468.

References

[1] B. Ren, W.A. Cassada, K.D. Wade, "Development of Deformation and Recrystallization Orientations during Hot Rolling of Al-4.5Mg Alloy," Materials Science Forum, Vol. 331-337, pp. 769-774, 2000.

[2] I.C. Hsiao and J.C. Huang. Metall. Mater. Trans. A, 2002, vol. 33A, 1373-84.

[3] P.A. Friedman and W.B. Copple: J. Mater. Eng. Perform., 2004, vol. 13, pp. 335-47.

[4] M.-A. Kulas, W.P. Green, E.M. Taleff, P.E. Krajewski, and T.R. McNelley, Metall. Mater. Trans. A, 2005, vol. 36A, pp. 1249-1261.

[5] I.C. Hsiao and J.C. Huang. Metall. Mater. Trans. A, 2002, vol. 33A, 1373-84.

[6] H. Kazama, K. Nakao, K. Takata, O. Noguchi, and Y. Suzuki: Proc. 108th Conf. of the Japan Institute of Light Metals (Light Metals Conf. 108th Spring Meeting), Japan Institute of Light Metals, Tokyo, 2005, pp. 61-62.

[7] F. Fukuchi, T. Yahaba, H. Akiyama, T. Ogawa, Hi. Iwasaki, and I. Hori: Honda R&D Tech. Rev., 2004, vol. 16, pp. 23-30.

[8] J.-K. Chang, K. Takata, K. Ichitani, and E.M. Taleff: Metall. Mater. Trans. A, 2010, vol. 41A, pp. 1942-53.

[9] E.O. Hall: Proc. Phys. Soc. B, 1951, vol. 64, pp. 747-53.

[10] N.J. Petch: J. Iron Steel Inst., 1953, vol. 174 pp. 25-28.

[11] D.J. Lloyd: Materials Forum, 2004, vol. 28, pp. 107-17.

[12] I. Samajdar, L. Rabet, B. Verlinden, and P. Van Houtte: Textures and Microstructures, 1998, vol. 30, pp. 191-206.

[13] S. Agarwal, P.E. Krajewski, and C.L. Briant: Metall. Mater. Trans. A, 2008, vol. 39A, pp. 1277-89.

[14] J.W. Bray, Aluminum Mill and Engineered Wrought Products, Properties and Selection: Nonferrous Alloys and Special-Purpose Materials, ASM Handbook, Vol. 2, ASM International, 1990, p 29–61.

[15] G.A. Henshall, M.E. Kassner, and H.J. McQueen: Metall. Trans. A, 1992, vol. 23A, pp. 881-89.

[16] W. Blum, Q. Zhu, R. Merkel, and H.J. McQueen: Mater. Sci. Eng., 1996, vol. A205, pp. 23-30.

[17] A. Gholina, F.J. Humphreys, and P.B. Prangnell: Acta Mater., 2002, vol. 50, pp. 4461–76.

[18] F.J. Humphreys and M. Hatherly: Recrystallization and Related Annealing Phenomena, Elsevier, New York, NY, 2004, pp. 461–65.

[19] G.F. Vander Voort, "Color Metallography", *Metallography and Microstructure*, ASM Handbook, Vol. 9, ASM International, 2004, pp. 493-512 (Figure 16).